Available online at www.sciencedirect.com
ScienceDirect
Coastal Engineering 55 (2008) 357–374
Coastal Engineering
An International Journal for Coastal, Harbour and Offshore Engineers
www.elsevier.com/locate/coastaleng

Combined classifier–quantifier model: A 2-phases neural model for prediction of wave overtopping at coastal structures

Hadewych Verhaeghe [a,*,1], Julien De Rouck [a], Jentsje van der Meer [b]

[a] Ghent University, Technologiepark 904, B-9052 Ghent, Belgium
[b] Van der Meer Consulting, P.O. Box 423, 8440 AK Heerenveen, The Netherlands

Received 3 July 2007; received in revised form 19 October 2007; accepted 5 December 2007
Available online 6 February 2008

Abstract

A 2-phases neural prediction method for wave overtopping is developed. The 'classifier' predicts whether overtopping occurs or not, i.e. $q=0$ or $q>0$. If the classifier predicts overtopping $q>0$, then the 'quantifier' is used to determine the mean overtopping discharge. The overtopping database set up within the EC project CLASH (De Rouck, J., Geeraerts, J., 2005. CLASH Final Report, Full Scientific and Technical Report, Ghent University, Belgium) is used to train the networks of the prediction method.

The method has an overall predictive capacity, and is able to distinguish negligible from significant overtopping, avoiding large overtopping overpredictions in the area of low overtopping. The prediction method is freely available on http://awww.ugent.be/awww/coastal/verhaeghe2005.html.

Keywords: Wave overtopping; Artificial neural network; Neural model; Prediction method; Coastal structures

1. Introduction and motivation

Coastal structures are designed to protect (often densely populated) coastal regions against wave attack, storm surges, flooding and erosion. The crest height plays a predominant role in the protective function of these structures. Due to climate changes, the sea level is rising at an increased rate, and storms substantially increase in intensity and duration (IPCC, 2007). This emphasises the importance of the design of these protective structures. The amount of sea water transported over the crest of a coastal structure, referred to as 'wave overtopping', is a critical design or safety assessment factor in this context.

Design of coastal structures should lead to an 'acceptable' overtopping amount. Which amount is assessed as acceptable is revealed by socio-economical reasons. High crested coastal structures preventing any overtopping are often very expensive. Moreover, such structures impose visual obstructions where the broad view on the sea is an important tourist attraction with an economical impact. However, the design of (lower crested) coastal structures should provide safety for people and vehicles on the structure, and avoid structural damage as well as damage to properties behind the structure. The preservation of the economical function of the structure under bad weather conditions is an additional important factor and has an influence on the design.

Various research on tolerable overtopping limits has been performed, resulting in guidance on allowable overtopping limits which provide safety for people and vehicles on the structure on the one hand, and structural safety on the other hand. Results of several studies are summarised in the Coastal Engineering Manual (U.S. Army Corps of Engineers, 2002) and more recently, in the Eurotop Assessment manual (Eurotop, 2007). Recent research on tolerable overtopping limits is performed within the CLASH project (Bouma et al., 2004 and Allsop, 2005).

There is a lack of reliable and robust prediction methods for wave overtopping at all kinds of coastal structures. Most frequently applied for structure design are empirical models, set up based on laboratory overtopping measurements. However,

* Corresponding author. Tel.: +32 92645489.
E-mail addresses: hadewych.verhaeghe@ugent.be (H. Verhaeghe), julien.derouck@ugent.be (J. De Rouck), jm@vandermeerconsulting.nl (J. van der Meer).
[1] Tel.: +32 92645489; fax: +32 92645837.

0378-3839/$ - see front matter © 2008 Elsevier B.V. All rights reserved.
doi:10.1016/j.coastaleng.2007.12.002

such models can only be applied within a restricted range (i.e. the test range of the data on which the model is based), and only a single structure configuration is covered. In addition, it is hard to find suitable prediction methods applicable for structures not having standard structure geometry. Finally models developed until now use a restricted number of wave parameters and structural parameters to predict mean overtopping discharges. The fact that each model is valid for only one specific structure type contributes to this. Considering various proposed overtopping models, it is seen that overtopping is influenced by many wave and structure characteristics.

Motivated by these findings, two generic prediction methods predicting wave overtopping at a variety of structure types and with an extensive range of applicability are developed. Both methods, developed at the same time, are trained with the extensive, screened overtopping database (Verhaeghe, 2005, Van der Meer et al., in press) set up within the CLASH project. Within the latter project Van Gent et al. (2007) developed a prediction method composed of a single neural model. The 2-phases neural prediction model described in this paper (see also Verhaeghe, 2005) is composed of two neural networks: a so-called 'classifier' followed by a so-called 'quantifier'.

The single CLASH network and the quantifier described in this paper are comparable; both networks are trained with a specific combination of data with measured overtopping discharge $q_{measured}>0$. In contrast to the CLASH network, the 2-phases neural model described in this paper is further developed also using data with $q_{measured}=0$. This has resulted in the classifier, able to distinguish negligible from significant overtopping, and to be used as filter for the quantifier.

It is shown in this paper that the use of 2 subsequent neural models has a significant added value versus the use of only 1 neural model: large overpredictions due to the inability of a single neural model to predict zero or small overtopping discharges are avoided.

In Section 2 a concise overall view is given of the various wave overtopping models which have been developed in the past. Further the overtopping database set up within the CLASH project is briefly discussed. In Section 3 the development of the 2-phases neural model is described in detail. After the overall methodology, the implications of the use of scale models for the development of an overtopping prediction method are treated. The development of the quantifier is discussed as third point in this section. Further the data which are used to train the classifier are examined, followed by the development of the classifier itself. In Section 4, four application examples are treated. Finally conclusions are drawn in Section 5.

2. Wave overtopping models and wave overtopping database

2.1. Wave overtopping models

Initial research on the overtopping phenomenon started in the 1950's. Saville (1955) was one of the first researchers to perform overtopping tests with regular waves. Ever since, overtopping research has gained more and more attention and several models to predict wave overtopping at different structures have been developed. Mainly physical model experiments provide the basic data for these models. During the first few decades overtopping was simulated in laboratories with regular waves only. Later on, irregular wave generation became standard, resulting in an improved accuracy of the developed prediction methods. The first well-known overtopping model based on irregular wave experiments in laboratory is the formula of Owen (1980). Even now, Owen's formula is used for the design of sloping structure types.

The most common approach to design coastal structures is to consider mean overtopping discharges q, expressed as flow rates per meter run ($m^3/s/m$ or l/s/m). Also limits for tolerable overtopping are most frequently expressed using mean overtopping discharges. A typical example are the 'guidelines for safety assessment for dikes' set up in the Netherlands by the Technical Advisory Committee on Flood Defence (TAW, 2002). The reason for the use of a 'mean' overtopping discharge is that this is a 'stable' parameter over about 1000 waves, in contrast to the volume of an individual overtopping wave.

Considering mean overtopping discharges, several types of overtopping models have been developed. The most important models can be summarised as follows:

- empirical models (=regression models)
  - ➢ simple regression models
  - ➢ weir-models
  - ➢ models based on run-up
  - ➢ graphical models
- numerical models

Empirical models are regression models, based on available overtopping data from physical model experiments. The first and most extensive examined group concerns simple regression models. Typically, in these models a relationship between a dimensionless discharge and a dimensionless crest freeboard is proposed, with certain parameters to be estimated starting from the available physical model tests. Typically, one concentrates on one specific structure type, which has resulted in overtopping models only applicable for vertical structures (a.o. Franco et al., 1994; Franco and Franco, 1999; Allsop et al., 1995) and in overtopping models only applicable for sloping structure types (a.o. Owen, 1980; TAW, 2002). Also for composite structure types overtopping models are developed (a.o. Ahrens et al., 1986; Ahrens and Heimbaugh, 1988). Nowadays simple regression models are still the basis of the design of many coastal structures. Weir-models are based on the weir analogy. Kikkawa et al. (1968) introduced this theoretical approach of overtopping. In models based on run-up, overtopping discharges are theoretically derived from run-up measurements. Some researchers present their results graphically, which leads to design diagrams for overtopping. The design diagrams of Goda (1985) are a well-known example.

Although empirical models are the most studied and applied models through the years, numerical models should also be mentioned. Numerical models simulate overtopping events in numerical wave flumes. Basically, the latter models solve a

series of differential equations describing fluid flow in front of and on the structure. The main disadvantage of numerical models is the huge amount of computation time which is required for precise models.

2.2. Wave overtopping database

As a consequence of the extensive study of wave overtopping over the last decades, large numbers of data sets on overtopping are widely spread over research institutes and universities all over the world. It concerns prototype overtopping measurements as well as many laboratory tests where overtopping at specific structures is measured. Within the CLASH project as much of these overtopping data were collected. In Table 1 the origin and nature of the collected data are summarised.

In total more than 10,000 overtopping data were gathered. All these data were put in a large database: 'the new overtopping database for coastal structures' (Verhaeghe 2005; Van der Meer et al., in press). This database, developed within the CLASH project and further referred to as the 'overtopping database', is used as the basis for the development of the 2-phases neural model.

As the aim of the set up of the overtopping database was to use it for multiple purposes, as much information as possible on each data set was searched for. Not only the raw data (wave parameters, geometry and corresponding overtopping discharges) were gathered, but also details of measurement methods (such as wave measurement methods and overtopping measurement methods) and analysis methods were collected. Each overtopping test is included in the database by means of 31 parameters. Eleven hydraulic parameters describe the wave characteristics and the wave overtopping. Seventeen structural parameters describe the test structure and 3 general parameters are related to general information about the overtopping test. The complexity factor CF and the reliability factor RF are two of these general parameters. They refer to the degree of approximation which is obtained by describing a test structure by means of the structural parameters in the database, respectively to the reliability of the considered overtopping test (Table 2). Further the database contains for part of the tests a remark and a reference to a report or paper describing the measurements.

The set-up of the overtopping database is described in Verhaeghe et al. (2003) and Steendam et al. (2004). Most detailed information can be found in Verhaeghe (2005), and in

Table 1
Origin and nature of tests in CLASH overtopping database

Country	Institution	Tests	M[1]	PT[2]
Belgium		(661)		
	– Flanders Community Coastal Division (FCCD)	11		11
	– Ghent University (UGent)	528	528	
	– Waterbouwkundig Laboratorium Borgerhout (WLB)	122	122	
Canada				
	– Canadian Hydraulics Centre (CHC)	225	225	
Denmark		(1390)		
	– Aalborg University (AAU)	1294	1294	
	– Danish Hydraulic Institute (DHI)	96	96	
Germany				
	– Leichtweiβ-Institut für Wasserbau (LWI)	1191	1191	
Iceland		39	39	
Italy (Modimar)		(1108)		
	– Enel-Hydro	309	309	
	– Estramed laboratory	126	126	
	– Modimar	194	117	77
	– University of Florence	479	479	
Japan		367	346	21
The Netherlands		(1247)		
	– Delta Marine Consultants (DMC)	64	64	
	– Delft Hydraulics (DH)	524	524	
	– Infram	659	659	
Norway		22	22	
Spain				
	– Universitat Politècnica de València (UPV)	284	284	
United Kingdom		(3211)		
	– Hydraulic Research Wallingford (HRW)	2177	2154	23
	– University of Edinburgh (UEDIN)	794	794	
	– Others	240	240	
United States				
	– Waterways Experiment Station (WES)	787	787	
TOTAL		**10532**	**10400**	132

[1]Model test.
[2]Prototype measurement.

Table 2
Meaning of values assigned to CF and RF

Value	Complexity factor CF	Reliability factor RF
1	Simple section The structural parameters describe the section exactly or as good as exactly	Very reliable test All needed information is available, measurements and analysis were performed in a reliable way
2	Quite simple section The structural parameters describe the section very well, although not exactly	Reliable test Some estimations/calculations had to be made and/or some uncertainties about measurements/analysis exist, but the overall test can be classified as reliable
3	Quite complicated section The structural parameters describe the section appropriate, but some difficulties and uncertainties appear	Less reliable test Some estimations/calculations had to be made and/or some uncertainties about measurements/analysis exist, leading to a classification of the test as less reliable
4	Very complicated section The section is too complicated to describe with the structural parameters, the representation of the section by these is unreliable	Unreliable test No acceptable estimations/calculations could be made and/or measurements/analysis include faults, leading to an unreliable test

Van der Meer et al. (in press). The final CLASH overtopping database is publicly available (Van der Meer et al., in press).

3. Development of a neural overtopping prediction method

3.1. Methodology

Artificial neural networks, often simply called neural networks (NNs), fall within the field of artificial intelligence. They can be defined as systems that simulate intelligence by attempting to reproduce the structure of human brains and can be trained on given input–output patterns. Typically, NNs consist of many inputs and outputs what makes these attractive for modelling multivariable systems and establishing nonlinear relationships between several variables in large databases. NNs have been applied successfully in various fields of coastal engineering research. The work by Mase et al. (1995), Van Gent and Van den Boogaard (1998), Medina (1999), Medina et al. (2002), Panizzo et al. (2003), Pozueta et al. (2004a) and Van Oosten and Peixo Marco (2005) can be mentioned in this context. The technique of using a 2-phases neural model has been proposed before by Medina (1998), to estimate run-up in dissipating basin breakwaters.

Both networks of the 2-phases neural model described in this paper are multilayer perceptrons (MLPs). They consist of multiple input parameters, one hidden layer with several hidden neurons and one output parameter. The single hidden layer is sufficient for the considered function approximation (universal approximation quality of NN's, Hornik, 1989). The output of both MLPs can be represented by:

$$y = \sum_{r=1}^{m} w_r \, f\left(\sum_{j=1}^{n} v_{rj} x_j + b_r\right) \tag{1}$$

with input $X \in \mathbb{R}^n$, output $y \in \mathbb{R}$, weight matrices $W \in \mathbb{R}^{1\times m}$, $V \in \mathbb{R}^{m\times n}$ en bias vector $\beta \in \mathbb{R}^m$, where n is the dimension of the input space, m is the number of neurons in the hidden layer and $\mathbb{R}$ is the set of real numbers.

Starting from a specific model structure, the NN problem is reduced to the determination of the unknown interconnection weights and biases. These parameters are established during the 'training' or 'learning' process. The MLPs are trained with data from the overtopping database using the Levenberg-Marquardt training algorithm (Levenberg, 1944; Marquardt, 1963). 'Bayesian optimalisation' of the parameters is applied, which ensures a good generalisation of the networks (Foresee and Hagan, 1997).

In a first attempt an optimal network configuration is determined for the neural classifier and quantifier. In both cases the selected data are split up in a random 'training set' (85%) and 'test set' (15%) for each network configuration. The training set is used to train the various models, whereas the test set is used to compare the performance of the developed models, using its root-mean-square error (rmse), defined as:

$$\text{rmse\_test} = \sqrt{\frac{1}{N_{\text{test}}}\sum_{n=1}^{N_{\text{test}}}\left[\left(o_{\text{test\_measured}}\right)_n - \left(o_{\text{test\_NN}}\right)_n\right]^2} \tag{2}$$

where N_{test} is the number of (weighed) test data, $O_{\text{test\_measured}}$ the wanted (i.e. measured) output and $O_{\text{test\_NN}}$ the output predicted by the network. The lower the value of rmse_test the better the overall prediction capacity of the considered network.

In a second attempt, the bootstrap technique is applied to the restrained optimal classifier and quantifier model configurations. The advantage of this resampling technique is that the entire data set can be used for the development of the final model. Originally, the bootstrap technique was introduced by Efron for determining the standard error of an estimator (Efron, 1982). In the bootstrap method subsets of the original data set are analysed, where a subset is generated by random selection *with replacement* from the original data set. The obtained bootstrap sets are each supposed to be a fair representative of the original data set, and of the entire input space. Several NNs, trained on the basis of different bootstrap sets, can be combined to reach a better, ensemble prediction, often called 'committees of networks'. If $f_b(x)$ refers to the model obtained by one bootstrap training b, and B to the total number of generated

bootstrap sets, then the prediction of the committee of networks, $f(x)$, is defined as:

$$f(x) = \frac{1}{B}\sum_{b=1}^{B} f_b(x) \quad (3)$$

The rationale is here that if each bootstrap network is biased for a particular part of the input space, the mean prediction over the ensemble of networks can reduce the prediction error significantly. Further the bootstrap technique allows to determine confidence intervals for the neural approximation. Efron and Tibshirani (1993) describe several methods to approximate confidence intervals with the bootstrap method. In this work bootstrap confidence intervals based on percentiles of the distribution of the bootstrap replications are considered. The 90% interval for the prediction $f(x)$ is determined by the smallest except 5% prediction $f_b(x)$ and the largest except 5% prediction $f_b(x)$ (with $b=1, \ldots, B$).

The use of 2 subsequent NNs for the neural overtopping prediction method instead of 1 single network originates from the approximately exponential relationship between measured overtopping discharge and crest freeboard of a structure (e.g. TAW, 2002). As a consequence, if a network is trained with non-preprocessed q-values as output, the network only performs well for the largest q-values ($q \approx 10^{-1}$m^3/s/m–10^{-2}m^3/s/m). Such network is not able to distinguish the smaller overtopping discharges from each other, as during the training process differences between $q_{measured}$ (=measured q-value) and q_{NN} (predicted q-value) are minimised.

A much better result is obtained when the output value q is preprocessed to its logarithm log(q) during training. Such network is also able to distinguish the smaller overtopping discharges, with equal relative errors for small and large overtopping discharges. Training a network with log(q) as output results in the quantifier in the first phase of the network development. However, as log(0) equals minus infinity, training on this preprocessed output suppresses the inclusion of data with $q=0$ m^3/s/m in the training data of the quantifier. As will be shown further in this paper, the consequence is that the quantifier does not generalise well for small and zero overtopping discharges. This finding resulted in the development of the classifier, able to classify overtopping as significant or negligible, and to be used as a filter for the quantifier. For the development of the classifier, the output parameter q is replaced by 2 discrete values, i.e. +1 and −1, referring to a situation with significant respectively negligible overtopping.

Only 17 of the 31 parameters included in the overtopping database are selected for the development of the neural overtopping prediction method. The selected parameters give a brief but complete overall view of an overtopping test. Table 3 lists these parameters, together with their function in the models.

In contrast to Van Gent et al. (2007), the authors prefer the use of the parameter 'B_h' (width of the horizontally schematised berm) over the use of the two parameters 'B' (width of the berm, measured horizontally) and '$\tan\alpha_B$' (tangent of angle that sloping berm makes with horizontal), as the (small number of) sloping berms included in the database concern only slightly inclined parts, and as an extra input parameter concerns a substantial increase of the neural model complexity.

Table 3
Database parameters selected for development of neural prediction method

Nature		Parameter		Function
Hydraulic	1	$H_{m0\ toe}$ [m]	(Wave height)	Input
	2	$T_{m-1,0\ toe}$ [s]	(Wave period)	Input
	3	β [°]	(Wave angle)	Input
	4	q [m3/s/m]	(Overtopping discharge)	Output
Structural	1	h [m]	(Water depth in front of structure)	Input
	2	h_t [m]	(Water depth on toe)	Input
	3	B_t [m]	(Width of toe)	Input
	4	γ_f [−]	(Roughness factor)	Input
	5	$\cot\alpha_d$ [−]	(Structure slope)	Input
	6	$\cot\alpha_u$ [−]	(Structure slope)	Input
	7	R_c [m]	(Crest freeboard)	Input
	8	h_b [m]	(Water depth on berm)	Input
	9	B_h [m]	(Berm width)	Input
	10	A_c [m]	(Armour freeboard)	Input
	11	G_c [m]	(Crest width)	Input
General	1	RF[−]	(Reliablility factor)	Weight factor
	2	CF[−]	(Complexity factor)	Weight factor

Fig. 1 shows a cross-section of a rubble mound structure with a berm. The 15 selected input and output parameters are marked. For detailed information on each parameter is referred to Verhaeghe (2005).

For the development of classifier and quantifier, the reliability factor RF and the complexity factor CF are combined into one 'weight factor', which gives an indication of the overall reliability of the test. The weight factor is determined as (Pozueta et al. (2004b)):

$$\text{weight factor} = (4 - \text{RF})*(4 - \text{CF}) \quad (4)$$

The value of the weight factor is linked to the number of times the corresponding test is used as input during the training and testing process. The more the same test is used as input during the training process, the more the trained NN will take account of the result of the corresponding test. This implies that the NN is forced to draw more attention to tests with high reliability and low complexity compared to tests with low reliability and high complexity. The most reliable tests are used 9 times as input. On the other side, unreliable tests or unreliably represented tests (i.e. RF=4 or CF=4) are not used for the development of the networks (~10% of all tests).

3.2. Implications of scale models

The overtopping database used as basis for the development of the prediction model is composed of model tests performed on different model scales as well as of prototype measurements. The laboratory tests are all models of (real or fictive) prototype situations, obtained by scaling the prototype situations according to the Froude model law.

To allow internal comparison of the tests, all tests are scaled according the Froude model law before using them as input-output patterns during the training of the NNs. The parameter

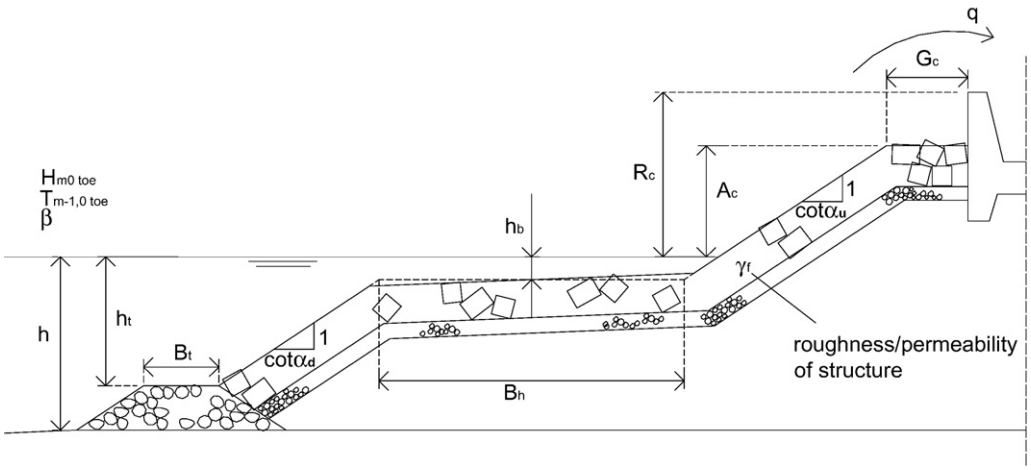

Fig. 1. Database input/output parameters selected for development of neural prediction method.

$H_{m0\ \mathrm{toe}}$ is used as length scale N_L for all input and output parameters, e.g. $R_c \rightarrow {}^{s}R_c = R_c / H_{m0\ \mathrm{toe}}$, $q \rightarrow {}^{s}q = q/(H_{m0\ \mathrm{toe}})^{3/2}$, … (scaled parameters are marked with an 's' in superscript before the parameter). This scaling procedure corresponds to the scaling of all tests to a fictive situation with a wave height $H_{m0\ \mathrm{toe}} = 1$ m. Consequently the parameter $H_{m0\ \mathrm{toe}}$ disappears as direct input parameter of the NNs.

For the parameters $\cot\alpha_u$, $\cot\alpha_d$, γ_f and β the value of the scaled parameter equals the original parameter, i.e. ${}^{s}\beta = \beta$, ${}^{s}\gamma_f = \gamma_f$, ${}^{s}\cot\alpha_u = \cot\alpha_u$ and ${}^{s}\cot\alpha_d = \cot\alpha_d$.

Overtopping studies within the CLASH project have shown that model and scale effects do affect overtopping measurements under certain circumstances, resulting in differences between prototype and model response. A quantification of these model and scale effects resulted in a 'scaling procedure' (the CLASH scaling procedure) to apply to overtopping measured during small scale tests (Kortenhaus et al., 2005). Further improvements to this scaling procedure are subject to research, see e.g. De Rouck et al., 2005).

As the majority of overtopping tests included in the database concern small scale overtopping tests, a neural prediction method for small scale overtopping is developed. To avoid confusion of the NNs, large scale tests (including prototype measurements), which would possibly be affected by model and scale effects if performed on a small scale, are excluded during the training of the neural models.

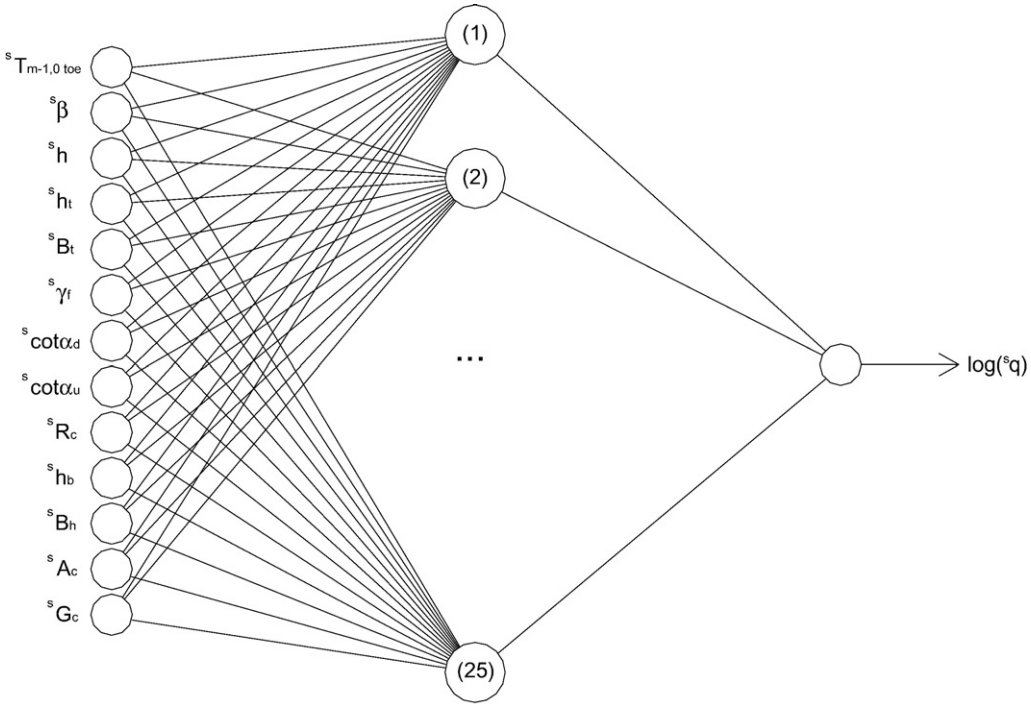

Fig. 2. Network architecture of overtopping quantifier.

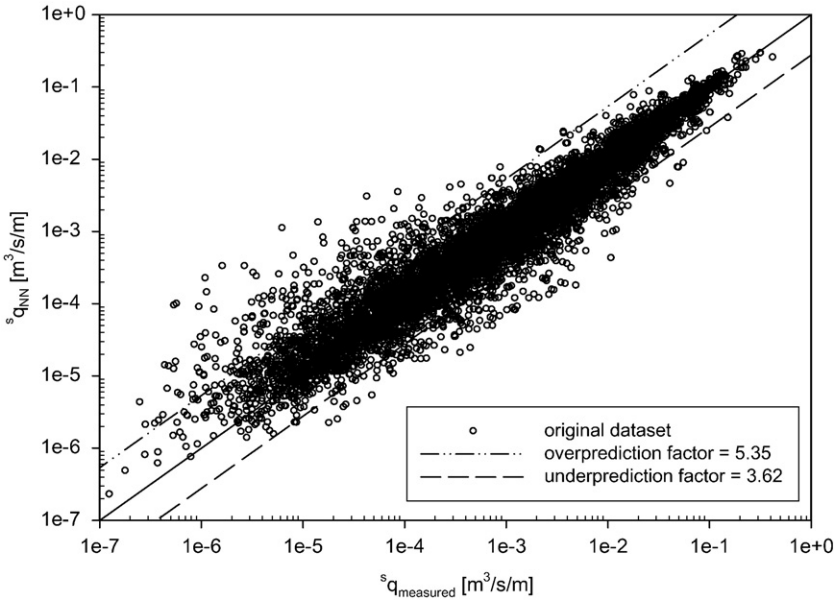

Fig. 3. Prediction by the committee of networks for the original data set (8195 data).

As the 2-phases neural model is a small scale model (comparable to many existing empirical models), one should apply a scaling procedure to the result to obtain the corresponding expected overtopping in prototype or at large scale.

3.3. Neural quantifier for quantification of significant overtopping

As the output of the quantifier is taken the logarithm of the (scaled) overtopping discharge, only overtopping data with $q>0$ m^3/s/m are used for the training of the quantifier. It concerns 8195 reliable overtopping tests (Van der Meer, in press), or 46328 'weighed' tests, i.e. the number of tests obtained when each test is multiplied by its weight factor. In contrast to Van Gent et al. (2007), also data with small q-values are assigned a weight factor according to Eq. (4). Although the relative error on such data is higher, a good 'mean prediction' of these data is obtained when using these. Moreover, using sufficiently data with small q-values is needed to allow the quantifier to learn to predict these small q-values.

The architecture of the neural quantifier is shown in Fig. 2. The network consists of 13 scaled input parameters, 1 hidden layer with 25 hidden neurons and 1 output parameter, i.e. log (^{s}q). The number of hidden neurons is determined by training several models, where the number of hidden neurons is varied. The performance of the models is compared for their test set (Eq.2), taking account of the fact that one extra hidden neuron corresponds to a significant increase of the network complexity. The multiplication of the data according to their weight factor is performed after splitting up the data in training and test set. This procedure leads to an independent test set, necessary to assess the model's performance.

The quantifier is further developed using the bootstrap method. One hundred bootstrap networks are trained on the basis of 100 bootstrap subsets. Each subset contains as many data as the original, weighed data set (i.e. 46328 data), and is sampled with replacement from the original, weighed data set. The bootstrap networks form a committee of networks (Eq. 3): a prediction with the quantifier is determined as the mean value of 100 predictions, obtained with the 100 bootstrap networks. Further for each prediction the 90% interval is given, calculated on the basis of the distribution of the bootstrap predictions.

Fig. 3 shows the final result of the committee of networks for the original data set. Predicted values $^{s}q_{NN}$ are represented versus measured values $^{s}q_{measured}$. The weighed rms-error equals 0.3100.

The performance of the quantifier for the original data set can also be assessed by means of the maximum error factors obtained for this data set. The error factor for overprediction ($^{s}q_{NN}>{}^{s}q_{measured}$) is defined as $^{s}q_{NN}/{}^{s}q_{measured}$, while the error factor for underprediction ($^{s}q_{NN}<{}^{s}q_{measured}$) is defined as $^{s}q_{measured}/{}^{s}q_{NN}$.

Table 4 shows the maximum error factors obtained when a specified percentage of the data is not considered. Considering $(100-x)$% of the data set, the $0.5*x$% largest factors for overprediction and the $0.5*x$ % largest factors for underprediction are not considered.

The maximum error factors obtained when 5% the data are omitted are marked in bold in Table 4. These values may be considered as a good indication of the general performance of the committee of networks.

As a NN is only able to predict well within the ranges of the data on which it was trained, and as in addition extrapolation of

Table 4
Maximum error factors for the original data set (weighed values)

% of data set considered	(100%)	99%	**95%**	90%
Maximum overprediction factor	(203.55)	31.35	**5.35**	3.34
Maximum underprediction factor	(27.48)	10.21	**3.62**	2.78

Table 5
Ranges of applicability for the quantifier

		$\gamma_f=1$			$\gamma_f<1$	
1	3.00	$\leq {}^{s}T_{m-1,0\ toe}$ [s] $\leq$	22.00	3.00	$\leq {}^{s}T_{m-1,0\ toe}$ [s] $\leq$	12.00
2	0	$\leq {}^{s}\beta$ [°] $\leq$	60.00	0	$\leq {}^{s}\beta$ [°] $\leq$	60.00
3	1.00	$\leq {}^{s}h$ [m] $\leq$	20.60	1.00	$\leq {}^{s}h$ [m] $\leq$	13.30
4	1.00	$\leq {}^{s}h_t$ [m] $\leq$	20.50	0.65	$\leq {}^{s}h_t$ [m] $\leq$	13.30
5	0	$\leq {}^{s}B_t$ [m] $\leq$	11.40	0	$\leq {}^{s}B_t$ [m] $\leq$	5.00
6	1.00	$\leq {}^{s}\gamma_f$ [−] $\leq$	1.00	0.35	$\leq {}^{s}\gamma_f$ [−] $\leq$	0.95
7	0	$\leq {}^{s}\cot\alpha_d$ [−] $\leq$	7.00	0	$\leq {}^{s}\cot\alpha_d$ [−] $\leq$	5.30
8	−5.00	$\leq {}^{s}\cot\alpha_u$ [−] $\leq$	6.00	0	$\leq {}^{s}\cot\alpha_u$ [−] $\leq$	8.00
9	0	$\leq {}^{s}R_c$ [m] $\leq$	5.00	0.25	$\leq {}^{s}R_c$ [m] $\leq$	2.80
10	−1.00	$\leq {}^{s}h_b$ [m] $\leq$	3.60	−1.00	$\leq {}^{s}h_b$ [m] $\leq$	1.20
11	0	$\leq {}^{s}B_h$ [m] $\leq$	16.20	0	$\leq {}^{s}B_h$ [m] $\leq$	6.20
12	0	$\leq {}^{s}A_c$ [m] $\leq$	4.00	0.10	$\leq {}^{s}A_c$ [m] $\leq$	2.90
13	0	$\leq {}^{s}G_c$ [m] $\leq$	7.60	0	$\leq {}^{s}G_c$ [m] $\leq$	5.40

a network outside these ranges may lead to pointless results, it is important to indicate ranges of applicability for the quantifier.

Table 5 shows the ranges of applicability determined for the quantifier. Structure types with a value of $\gamma_f=1$ are distinguished from structure types with a value of $\gamma_f<1$, which corresponds approximately to the distinction between smooth structure types and rough structure types. The parameter ranges are chosen in this way that outliers are excluded.

The data with $q_{measured}=0$ m^3/s/m in the overtopping database can be used to check if the quantifier is able to generalise for the trend of zero overtopping (Table 6, *single quantifier simulation*). Low values for ${}^{s}q_{NN}$ should be predicted by the quantifier for these data, i.e. preferably lower than approximately 10^{-6} m^3/s/m. The number of reliable and 'precise' data with $q_{measured}=0$ m^3/s/m is 657 (3521 weighed data). Herewith 'precise' refers to an accurate measurement system, assuring that zero overtopping measurements really concern zero or at least negligible discharges. Almost half of the weighed zero data (43.06%) have at least one of the input parameters outside the ranges of applicability of the quantifier. A reason for this high percentage is that zero measurements are often caused by specific combinations of parameters on which the quantifier has not been trained. These data can not be simulated by the quantifier (at least not with a reliable result). The results of the simulation of the remaining 56.94% of the weighed zero data (i.e. 2005) are represented in Table 6 (*single quantifier simulation*).

Table 7
Reliable and precise data for development of the classifier

	Original Database	Weighed Database
Total # reliable and precise data	8852	49849
of which		
# data in class−1	698	3710
of which		
# data with ${}^{s}q_{measured}=0$ m^3/s/m	657	3521
# data in class+1	8154	46139

In contrast to what might be expected, Table 6 (*single quantifier simulation*) shows that the majority of the quantifier simulations of zero overtopping measurements results in quite high overtopping predictions. Values of ${}^{s}q_{NN}$ even larger than 10^{-3} m^3/s/m occur. This result shows that the quantifier is not able to generalise for overtopping discharges $q=0$ m^3/s/m, which was the direct boost for the development of the classifier as filter for the quantifier.

3.4. Data for development of the classifier

As the classifier only has to classify overtopping as $q=0$ or $q>0$, the output value of the classifier is restricted to two possible values: +1 = significant overtopping (further referred to as class+1) and −1 = (zero or) negligible overtopping (further referred to as class−1). The limit of significant overtopping is set to ${}^{s}q=10^{-6}$ m^3/s/m, i.e. all data with ${}^{s}q_{measured}<10^{-6}$ m^3/s/m are assigned to class−1. Table 7 shows the available data for development of the classifier.

Two reasons may be quoted for the fact that the number of zero data is quite low compared to the non-zero data.

The first reason is that researchers performing overtopping tests are more interested in non-zero overtopping measurements (e.g. to compare with admissible overtopping rates) than in data where no overtopping is measured. Many researchers simply do not report their zero measurements.

The second reason can be attributed to the fact that many laboratories perform parametric tests, which are stopped once

Table 6
Values of ${}^{s}q_{NN}$ for simulation of zero data by single quantifier/combined classifier–quantifier

	Single quantifier simulation	Combined classifier-quantifier simulation
	% of all zero data (3521 weighed data)	% of all data from class−1 (3710 weighed data)
(Input out of range)	(43.06)	(1.07)
${}^{s}q_{NN}>10^{-6}$ m^3/s/m of which	54.50	18.22
${}^{s}q_{NN}>10^{-2}$ m^3/s/m	(1 wrong zero measurement: 0.09)	0
10^{-2} m^3/s/m $\geq {}^{s}q_{NN}>10^{-3}$ m^3/s/m	1.53	0.97
10^{-3} m^3/s/m $\geq {}^{s}q_{NN}>10^{-4}$ m^3/s/m	7.36	4.19
10^{-4} m^3/s/m $\geq {}^{s}q_{NN}>10^{-5}$ m^3/s/m	28.40	11.63
10^{-5} m^3/s/m $\geq {}^{s}q_{NN}>10^{-6}$ m^3/s/m	17.12	1.42
${}^{s}q_{NN}\leq 10^{-6}$ m^3/s/m	2.44	0
Total	100.00	19.29

no overtopping is measured anymore. In a parametric test series, the influence of one or some parameters is studied, keeping the remaining test configuration unchanged. Examples are tests where the crest height of a structure is varied. The moment no significant overtopping is measured anymore, the test series is often stopped, as the researcher knows for sure that higher crest levels will result in more zero measurements. Few zero values in the overtopping results is then a consequence. Another consequence is that only near the border of overtopping — no overtopping, zeros are included in the database, although it is known that for e.g. larger crest heights also zero overtopping would be measured. Consequently it may be expected that the data from class−1 only constitute a part of the entire 'negligible overtopping' space, i.e. the data included in class−1 are not a representative sample for all possible negligible overtopping measurements. By developing a classifier on these restricted zero values only, classifying problems will raise for e.g. crest heights which are slightly higher than the value corresponding to a zero measurement for a specific structure.

To force the classifier to pay as much attention to the negligible overtopping data as to the significant overtopping data, a comparable number of data from both classes should be used to develop the model (see Medina et al., 2002). To avoid a huge loss of information by not using the majority of available data for class+1 and in addition to improve the problem of the bad distribution of the data within the entire 'negligible overtopping'-space, the number of data in class−1 is increased by creating artificial zero data. The available zero measurements are used as a starting point, and the zero space is extended in two directions:

- artificial data with higher values of ${}^{s}R_c$ are added and
- artificial data with higher values of ${}^{s}G_c$ are added.

By adding artificial data with higher ${}^{s}R_c$ and ${}^{s}G_c$-values, the zero space is only filled in two single directions. More parameters can be thought of which could, by increasing or decreasing their value, result in more zero data. However, only the parameters ${}^{s}R_c$ and ${}^{s}G_c$ are used in this work. Artificial data with higher ${}^{s}R_c$ values are emphasised.

The first set of artificial zero data is created by copying the input parameters of the available zero measurements, except for the value of ${}^{s}R_c$, which is raised. Inextricably bound up with this is an increase of the value of ${}^{s}A_c$ (Fig. 4). If the value of ${}^{s}R_c$ is multiplied by $(1+x)$, with $x>0$, the value of ${}^{s}A_c$ increases by a factor $[1+x*({}^{s}R_c/{}^{s}A_c)]$. Increasing the value of ${}^{s}A_c$ as well corresponds to extending the middle part of the structure, keeping the crest configuration unchanged.

The second set of artificial zero data is created by copying the input parameters of the original zero measurements once more, and raising only the value of ${}^{s}G_c$. Multiplying the ${}^{s}G_c$-value with a factor $(1+y)$, with $y>0$, does not request changes to additional input parameters.

Examination of several combinations of factors x and y led to following final values used for the extension of the data from class−1:

$$\text{value of } x \text{ in} (1+x)*{}^{s}R_c : \ 0.1/0.2/0.3/0.5$$

$$\text{value of } y \text{ in} (1+y)*{}^{s}G_c : \ 0.2/0.5$$

Adding these artificial data to the original number of 698 data in class−1, this results in a new number of (original) data in class−1 of 4206 (22550 weighed data).

3.5. Neural classifier for classification of q as negligible or significant overtopping

The optimal network configuration is determined by training and testing the classifier with a (weighed) training set respectively a (weighed) test set. The latter sets are determined by first assembling the 4206 available (non-weighed) data in class−1 and an equal number of data randomly taken from the (non-weighed) 8154 data in class+1. Only after splitting up

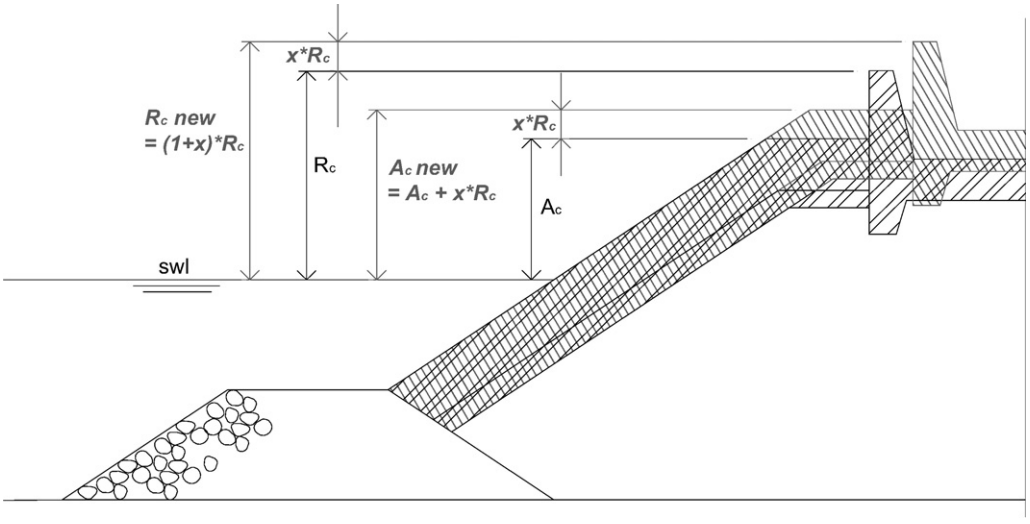

Fig. 4. Creation of artificial data by raising the value of R_c (and A_c).

Table 8
Values of ${}^{s}q_{measured}$ corresponding with wrongly classified data from class+1 by classifier

Values of ${}^{s}q_{measured}$	% wrongly classified (of 46139 data)
${}^{s}q_{measured} > 10^{-2}$ m^3/s/m	0
10^{-2} m^3/s/m $\geq {}^{s}q_{measured} > 10^{-3}$ m^3/s/m	0.02
10^{-3} m^3/s/m $\geq {}^{s}q_{measured} > 10^{-4}$ m^3/s/m	0.29
10^{-4} m^3/s/m $\geq {}^{s}q_{measured} > 10^{-5}$ m^3/s/m	0.99
10^{-5} m^3/s/m $\geq {}^{s}q_{measured} > 10^{-6}$ m^3/s/m	0.50
TOTAL:	1.80

these assembled data in a training and test set, the data are multiplied according to their weight factor.

The architecture of the overtopping classifier is similar to that of the quantifier (Fig. 2). As both networks are meant to function in series, the input layer of the classifier consists of the same 13 input parameters as the input layer of the final quantifier. The output of the classifier logically differs from the quantifier output, and can adapt only 2 possible values, i.e. +1 for significant overtopping and −1 for negligible overtopping. The number of hidden neurons is determined to be 20.

The classifier is further developed using the bootstrap method. Sixty-one bootstrap networks are trained on the basis of 61 bootstrap subsets, each containing 45,100 data (22,550 data from class−1 and 22,550 data from class+1). The 61 bootstrap networks are used to determine an optimal decision border for the classification of a data point to class+1 or −1. Based on the observation that the wrongly classified data from class+1 concern rather high values of ${}^{s}q_{measured}$, and considering the important aspect of safety in overtopping design, a selection criterion which gives priority to minimise the number of wrongly classified non-zero data is chosen: a data point is assigned to class+1 if more than 5 bootstrap models predict class+1. The criterion allows for some models to lead to bad predictions in some parts of the input space due to local scarce occupation, without causing consequent overprediction of overtopping.

Of all available reliable weighed data from the overtopping database (i.e. 49849 data, see Table 7), 3.09% is wrongly classified by the classifier. This corresponds to a misclassification of less than 20% of the data from class−1, versus a misclassification of only 1.80% of the data from class+1. Table 8 gives an overall view of the nature of the misclassifications of the data from class+1.

As the goal of the classifier is to serve as filter for the data to be put into the quantifier, all data assessed by the classifier as +1, i.e. showing significant overtopping, have to be simulated by the quantifier to obtain a prediction of the value of the overtopping discharge. The results of the quantifier simulation of the wrongly classified data from class−1 (19.29%), ${}^{s}q_{NN}$, are given in Table 6 (combined classifier–quantifier simulation).

Due to the choice of a strict selection criterion for class−1, data which are on the border of zero overtopping will be inclined to be classified as non-zero overtopping, (sometimes) leading to rather high overtopping discharges predicted by the quantifier.

However, compared to the single quantifier performance, the number of overtopping overpredictions is significantly reduced using the classifier. In Fig. 5 (see also Table 6) the prediction performance of the combined classifier–quantifier (black italic) is compared with the prediction performance of the single quantifier (grey italic), for the available data in class−1. The numbers are

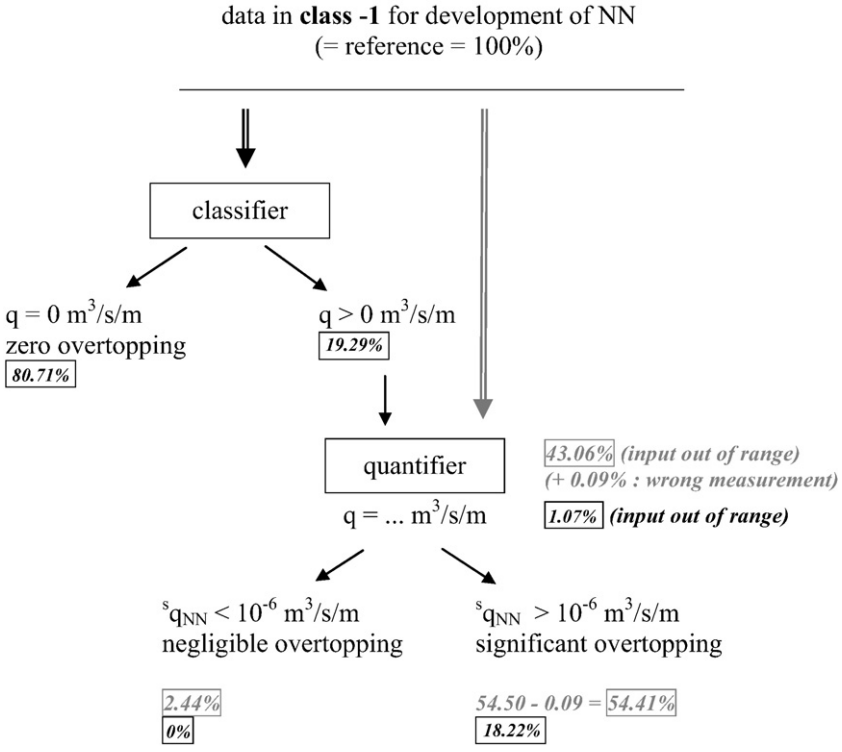

Fig. 5. Performance of single quantifier (grey italic) versus performance of combined classifier–quantifier (black italic) for data in class−1.

Table 9
Ranges of applicability for the classifier

	$\gamma_f = 1$			$\gamma_f < 1$		
1	3.00	$\leq {}^{s}T_{m-1,0\ toe}$ [s] $\leq$	22.00	3.00	$\leq {}^{s}T_{m-1,0\ toe}$ [s] $\leq$	12.00
2	0	$\leq {}^{s}\beta$ [°] $\leq$	60.00	0	$\leq {}^{s}\beta$ [°] $\leq$	60.00
3	1.00	$\leq {}^{s}h$ [m] $\leq$	20.60	1.00	$\leq {}^{s}h$ [m] $\leq$	13.30
4	1.00	$\leq {}^{s}h_t$ [m] $\leq$	20.50	0.65	$\leq {}^{s}h_t$ [m] $\leq$	13.30
5	0	$\leq {}^{s}B_t$ [m] $\leq$	11.40	0	$\leq {}^{s}B_t$ [m] $\leq$	5.00
6	1.00	$\leq {}^{s}\gamma_f$ [−] $\leq$	1.00	0.35	$\leq {}^{s}\gamma_f$ [−] $\leq$	0.95
7	0	$\leq {}^{s}\cot\alpha_d$ [−] $\leq$	7.00	0	$\leq {}^{s}\cot\alpha_d$ [−] $\leq$	5.30
8	−5.00	$\leq {}^{s}\cot\alpha_u$ [−] $\leq$	6.00	0	$\leq {}^{s}\cot\alpha_u$ [−] $\leq$	8.00
9	0	$\leq {}^{s}R_c$ [m] $\leq$	7.50	0.25	$\leq {}^{s}R_c$ [m] $\leq$	4.20
10	−1.00	$\leq {}^{s}h_b$ [m] $\leq$	3.60	−1.00	$\leq {}^{s}h_b$ [m] $\leq$	1.20
11	0	$\leq {}^{s}B_h$ [m] $\leq$	16.20	0	$\leq {}^{s}B_h$ [m] $\leq$	6.20
12	0	$\leq {}^{s}A_c$ [m] $\leq$	6.00	0.10	$\leq {}^{s}A_c$ [m] $\leq$	4.35
13	0	$\leq {}^{s}G_c$ [m] $\leq$	11.40	0	$\leq {}^{s}G_c$ [m] $\leq$	8.10

expressed in percentages of the total number of data. Although the results for the combined classifier–quantifier refers to 3710 weighed negligible overtopping data, whereas the results for the single quantifier only refer to the zero overtopping measurements, i.e. 3521 weighed data, the percentages give an idea of the significantly better performance of the combination classifier–quantifier. It has been found in Table 6 that (54.50%–0.09%)= 54.41% of the considered zero data are predicted by the single quantifier as ${}^{s}q_{NN} > 10^{-6}$ m^3/s/m. The use of the classifier reduces the quantifier predictions ${}^{s}q_{NN} > 10^{-6}$ m^3/s/m to 18.22% of the considered zero data. This is a reduction of approximately a factor 3. In addition, the percentage of zero overtopping measurements for which no overtopping prediction can be given, decreases from 43.06% for the single quantifier, to only 1.07% if the classifier is used as filter for the quantifier. The classifier classifies (100%–19.29%)=80.71% of the considered zero overtopping measurements correctly as negligible overtopping.

This noticeably better prediction of the zero overtopping measurements when using the classifier as a filter for the quantifier has as negative consequence the classification of 1.80% of the non-zero measurements as zero. However, this percentage is very low and is therefore considered as acceptable.

Analogous to the quantifier, ranges of applicability are defined for the classifier. As the data set on which the classifier has been trained, encloses the data set on which the quantifier has been trained, the minimum/maximum-intervals for individual input parameters of the classifier are at least evenly wide as these of the quantifier. The classifier has not only been trained on extra zero measurements, but especially the artificially created zero data enlarge the ranges of applicability: the maximum values for the input parameters ${}^{s}R_c$, ${}^{s}A_c$ and ${}^{s}G_c$ are multiplied with a factor 1.5 (Table 9). This factor originates from the methodology applied to create the artificial data, where the input parameters ${}^{s}R_c$ and ${}^{s}G_c$ were multiplied with a maximum factor of 1.5.

Analogous to the quantifier, new input for the classifier should always be situated within the given ranges of applicability.

4. Application examples

In this section, the 'combined classifier–quantifier predictions' are discussed for some specific test series.

In Section 4.1 and Section 4.2 the 2-phases neural model is applied to two artificial test series of which the overtopping discharge can be estimated quite accurately with available empirical formulae. It concerns overtopping at a rubble mound structure and at a vertical wall.

In Section 4.3 and Section 4.4 the 2-phases neural model is used for the simulation of overtopping at a prototype site in Ostia (Italy) respectively at a prototype site in Zeebrugge (Belgium). As the prediction model concerns a small scale prediction method, a scaling procedure is applied to these results, allowing comparison with the real measured overtopping values.

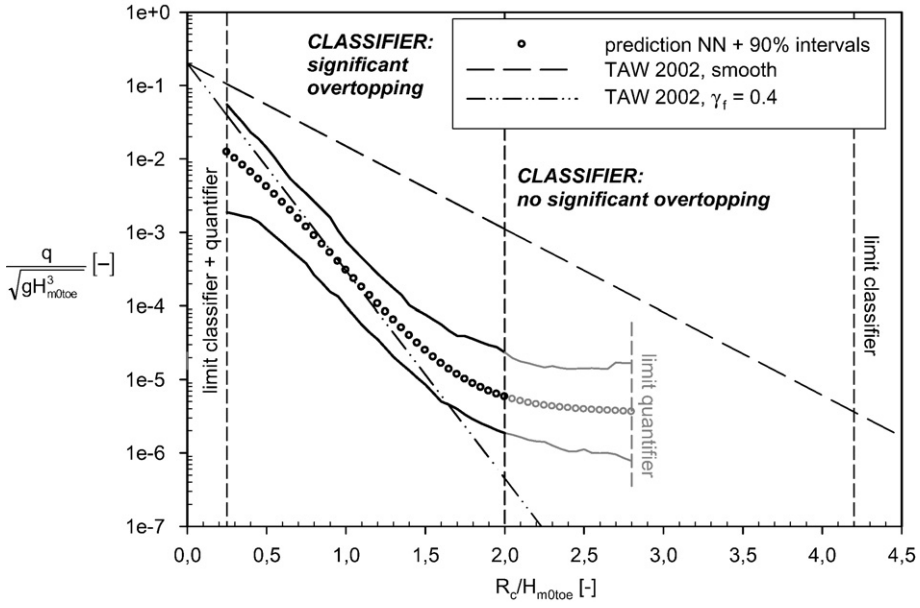

Fig. 6. Combined classifier–quantifier prediction of overtopping at rubble mound structure with rocks.

4.1. Application example 1: overtopping at a rubble mound structure

An artificial data set on wave overtopping at a rubble mound structure has been generated, and the predicted overtopping by the 2-phases neural model is compared with an existing deterministic formula. Following wave and structure characteristics are considered: ${}^{s}\beta=0°$ (perpendicular wave attack), ${}^{s}T_{m-1,0\ \mathrm{toe}}=4.91$ s (corresponding to a wave steepness $s_0=0.043$), ${}^{s}h=7.14$ m, the armour is supposed to consist of 2 layers of rock, i.e. $\gamma_f=0.4$ (Verhaeghe, 2005), and the slope of the structure is supposed to equal 1:2. ${}^{s}G_c$ is supposed to be equal to 0.9 m (approximately 3 armour units).

The classifier simulation is performed for values of $0.25\ \mathrm{m} \le {}^{s}R_c \le 4.2$ m (see Table 9). The classifier predicts negligible overtopping for values of ${}^{s}R_c > 2$ m. For values of ${}^{s}R_c \le 2$ m consistent significant overtopping is predicted. In Fig. 6 the combined classifier–quantifier predictions+90% intervals are shown. For comparison the TAW-line for smooth dikes and the TAW-line for rough structure slopes with $\gamma_f=0.4$ are represented (TAW, 2002).

The quantifier predictions which are obtained for values of ${}^{s}R_c > 2$ m are represented in Fig. 6 in grey. However, as the classifier predicts negligible overtopping for these crest heights, the corresponding quantifier predictions should not be considered. The outcome of the combined classifier–quantifier network can thus be summarised as follows:

- The classifier only predicts significant overtopping at the considered rubble mound structure under above specified wave attack for values of $0.25\ \mathrm{m} \le {}^{s}R_c \le 2$ m. For values of $2\ \mathrm{m} < {}^{s}R_c \le 4.2$ m no significant overtopping is expected. For values of ${}^{s}R_c > 4.2$ m and values of ${}^{s}R_c < 0.25$ m the classifier is not able to make a reliable classification.
- For values of $0.25\ \mathrm{m} \le {}^{s}R_c \le 2$ m the quantifier can be used to predict values for the overtopping discharges. The results are represented in Fig. 6.

The predicted overtopping discharge by the final model is slightly higher for values of ${}^{s}R_c > 1.2$ m than the values obtained with the TAW-formula. For values of ${}^{s}R_c < 0.8$ m the quantifier predicts slightly lower values compared to the ones obtained with the TAW-formula. The latter trend is in accordance with the findings of Schüttrumpf (2001) who investigated overtopping at smooth slopes for zero crest freeboard. The 90% intervals are smallest for values of ${}^{s}R_c = 0.5$ m à 1.5 m. The percentile intervals show that the quantifier encounters more uncertainties for the smallest and largest values of ${}^{s}R_c$, corresponding to ${}^{s}R_c$-values in the vicinity of the limit of applicability.

In case the classifier would not be used as filter for the quantifier, the prediction would be very poor for large ${}^{s}R_c$-values. Fig. 6 shows that for large ${}^{s}R_c$-values, the quantifier keeps predicting quite high values of the dimensionless overtopping discharge, whereas a trend to zero overtopping is expected (comparable to the predictions by the TAW-formula). The quantifier has difficulties to predict dimensionless overtopping discharges $\frac{q}{\sqrt{gH_{m0\mathrm{toe}}^3}}$ lower than $\approx 10^{-5}$–10^{-6}. In a prototype situation with $H_{m0\ \mathrm{toe}}=3$ or 5 m the value of 10^{-5} corresponds to $q \approx 1.5 * 10^{-4}$ m^3/s/m respectively $q \approx 3.5 * 10^{-4}$ m^3/s/m.

It is very clear from Fig. 6 that the obtained overtopping prediction with the combination classifier–quantifier is a significant improvement over the result obtained by the quantifier only.

4.2. Application example 2: overtopping at a vertical wall

An artificial data set on wave overtopping at a vertical wall is generated, and the predicted overtopping by the 2-phases neural

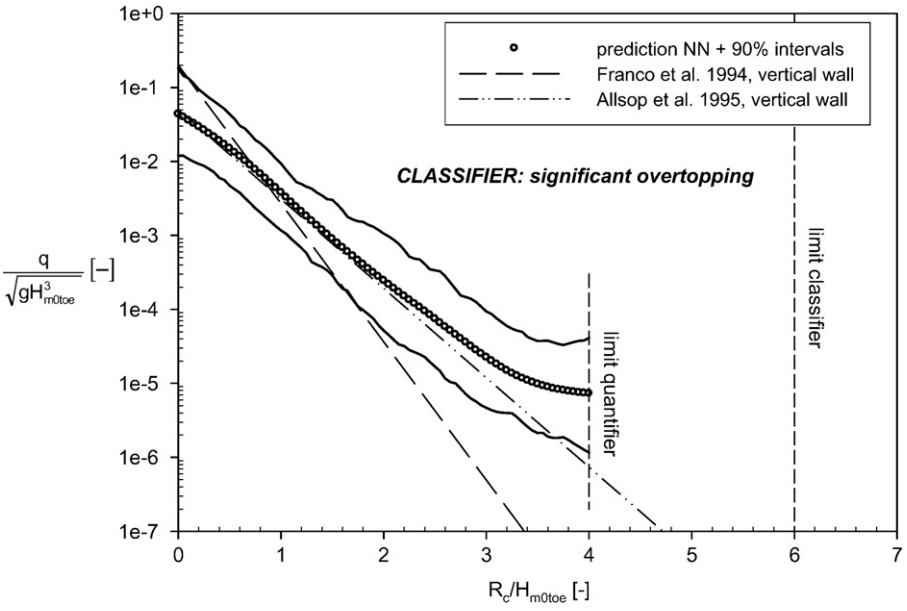

Fig. 7. Combined classifier–quantifier prediction of overtopping at vertical wall.

model is compared with existing deterministic formulae. Following wave and structure characteristics are considered: ${}^{s}\beta=0°$ (perpendicular wave attack), ${}^{s}T_{m-1,0\ \mathrm{toe}}=4.91$ s (corresponding to a wave steepness $s_0=0.043$), ${}^{s}h=7.14$ m, ${}^{s}G_c=0$ m.

The classifier simulation is performed for values of $0\ \mathrm{m}\le {}^{s}R_c\le 6$ m (see Table 9). The classifier predicts negligible overtopping for values of ${}^{s}R_c>6$ m. For values of ${}^{s}R_c\le 6$ m consistent significant overtopping is predicted. In Fig. 7 the combined classifier–quantifier predictions+90% intervals are shown. For comparison the formulae of Franco et al. (1994) and of Allsop et al. (1995) are represented. Both formulae are set up for overtopping at vertical walls in relatively deep water, which is in accordance with the considered artifical data set.

The outcome of the combined classifier–quantifier network can be summarised as follows:

- Overtopping at the considered vertical wall under previously specified wave attack may be expected for values of ${}^{s}R_c$ up to 6 m. For higher values of ${}^{s}R_c$ the classifier is not able to make a reliable classification.
- The predictions obtained with the quantifier for values of $0\ \mathrm{m}\le {}^{s}R_c\le 4$ m are shown in Fig. 6. For values of $4\ \mathrm{m}<{}^{s}R_c\le 6$ m, it is only known that overtopping may be expected, but no reliable discharges can be quantified with the developed model as ${}^{s}R_c=4$ m is the limit of applicability of the quantifier.

The quantifier prediction follows the line proposed by Allsop et al. (1995) very well for values of ${}^{s}R_c<3$ m. For larger values of ${}^{s}R_c$ the quantifier predicts slightly higher overtopping discharges. The same remark as for the previous data set can be made here, i.e. the quantifier seems to have difficulties predicting low overtopping discharges.

In contrast to the sloping structure considered in Section 4.1, also small 90% intervals are obtained for values of ${}^{s}R_c=0$ m. The availability of overtopping tests with vertical walls where $R_c=0$ m in the database explains this.

4.3. Application example 3: prototype overtopping at the Ostia breakwater

In Ostia (Italy, near Rome) prototype overtopping was measured at a rubble mound breakwater armoured with rocks.

Fig. 8. Ostia measurement site (courtesy prof. Franco).

Table 10
Ranges of input parameters of prototype data for neural prediction model

	Ostia breakwater	Zeebrugge breakwater
${}^{s}T_{m-1,0\ \mathrm{toe}}$ [s]	4.57–6.66	3.60–3.77
${}^{s}\beta$ [°]	1.00–40.00	0
${}^{s}h$ [m]	1.74–2.32	2.28–3.65
${}^{s}h_t$ [m]	1.74–2.32	1.87–3.04
${}^{s}B_t$ [m]	0	2.66–4.01
${}^{s}\gamma_f$ [−]	0.40	0.47
${}^{s}\cot\alpha_d$ [−]	4.00	1.40
${}^{s}\cot\alpha_u$ [−]	4.00	1.40
${}^{s}R_c$ [m]	1.72–2.56	1.37–2.30
${}^{s}h_b$ [m]	0	0
${}^{s}B_h$ [m]	0	0
${}^{s}A_c$ [m]	1.72–2.56	1.89–3.01
${}^{s}G_c$ [m]	2.00–2.75	1.33–2.01

In Fig. 8 a picture of overtopping at the Ostia breakwater is represented. Detailed information on the Ostia prototype site and the corresponding measurements is given in Franco et al. (2004 and in press).

There are 77 prototype overtopping measurements available at Ostia, originating from 7 measured storms (2003–2004), of which the overtopping results are processed per hour. For the measured mean wave periods $T_{m\ \mathrm{toe}}\approx 6$–9 s; this corresponds to processing overtopping events per 600 à 400 waves. Especially for the longer waves ($T_{m\ \mathrm{toe}}\approx 9$ s) this processing time is rather short.

The needed scaled hydraulic and structural parameters are determined for all 77 data, leading to values (ranges) of the input parameters for the neural prediction model as summarised in Table 10.

All data fall within the ranges of applicability of the classifier. Eight of the 77 data are assessed by the classifier as negligible overtopping in small scale tests, versus 69 as significant overtopping. As all these 69 data fall within the ranges of applicability of the quantifier, 69 (small scale) overtopping predictions ${}^{s}q_{\mathrm{NN}}$ are obtained.

Before comparison with the prototype measurements is possible, the predictions are to be corrected for expected model and scale effects. According to De Rouck et al. (2005) significant model and scale effects are expected for rough, flat breakwater slopes:

$$q_{\mathrm{proto}} = q_{\mathrm{ss}} * f_{\mathrm{scale\_wind}} \tag{5}$$

with

q_{proto}=prototype wave overtopping discharge in $\mathrm{m}^3/\mathrm{s/m}$

q_{ss}=wave overtopping discharge in $\mathrm{m}^3/\mathrm{s/m}$ originating from small scale model test which has been scaled to prototype result using Froude ($q_{\mathrm{small\_scale}}$)

$f_{\mathrm{scale\_wind}}$=scale factor accounting for possible scale and wind effects for rough, flat breakwater slopes:

$$\text{for } q_{\mathrm{ss}}<1.10^{-5}\mathrm{m}^3/\mathrm{s/m}: f_{\mathrm{scale\_wind}}=24$$

$$\text{for } 1.10^{-5}m^3/s/m\le q_{\mathrm{ss}}\le 1.10^{-2}\mathrm{m}^3/\mathrm{s/m}:$$

$$f_{\mathrm{scale\_wind}}=1+23.\left(\frac{-\log q_{\mathrm{ss}}-2}{3}\right)^3$$

$$\text{for } q_{\mathrm{ss}}>1.10^{-2}m^3/s/m: f_{\mathrm{scale\_wind}}=1$$

The (small scale) predicted values ${}^{s}q_{NN}$ by the quantifier can be corrected with formula (5) by first scaling up to prototype with Froude, i.e. $q_{NN}=q_{ss}={}^{s}q_{NN}*(H_{m0\ toe})^{3/2}$.

For the 8 data points classified as negligible overtopping, the scaling procedure (5) cannot be applied (zero overtopping remains zero overtopping). A procedure was developed to determine a small non-zero prototype overtopping discharge in these cases. The rationale is that the zero is obtained through the limited measurement accuracy present in small scale tests. The procedure uses available non-zero q-values of the same test series (i.e. identical structure geometry) with comparable wave characteristics, to estimate small non-zero q-values corresponding to the zero small scale results.

The starting point is a graph with the dimensionless overtopping discharge $\frac{q}{\sqrt{gH^3_{m0\ toe}}}$ versus the dimensionless crest height $R_c/H_{m0\ toe}$ (or armour height $A_c/H_{m0\ toe}$, depending on the structure geometry) where an empirical formula is fitted through the non-zero q-values. Starting from the value of $R_c/H_{m0\ toe}$ (or $A_c/H_{m0\ toe}$) of the test with $q=0$ m^3/s/m, the empirically predicted value $\frac{q_{ss\_est}}{\sqrt{gH^3_{m0\ toe}}}$ is determined, resulting in a (small) estimated value of q, i.e. q_{ss_est}. The correction for model and scale effects (formula (5)) can then be applied, starting from this small non-zero estimation q_{ss_est}.

Fig. 9 shows the procedure applied for the Ostia data points. The best matching TAW prediction line (TAW, 2002) corresponds to a value of $\gamma_f=0.38$.

The outcome of the combined classifier–quantifier model for the Ostia data can be summarised as follows (Fig. 10):

- Eight of the 77 prototype data are assessed by the classifier as resulting in negligible overtopping in small scale tests. As the aim of the simulation is to obtain a prototype prediction, a procedure to estimate prototype predictions from zero small scale predictions is applied. The estimations for the zero predictions all concern values of ${}^{s}q_{ss\_est}\le 10^{-6}$ m^3/s/m.
- Applying a scaling factor f_{scale_wind} to the 8 converted zero predictions q_{ss_est} and to the 69 quantifier predictions q_{NN}, results in values of ${}^{s}q_{NN\_corr\_final}$ as represented in the figure. The rms-error of the final corrected network prediction ${}^{s}q_{NN\_corr\_final}$ is found to be 0.5249.
- For the final corrected values ${}^{s}q_{NN\_corr\_final}$ originating from the quantifier predictions the 90% intervals are given. They are calculated by correcting the 90% values obtained for the original results ${}^{s}q_{NN}$ for the expected model and scale effects.

One can see that the corrected values result in a rather good match between the predictions and the prototype measurements, although for small values of ${}^{s}q_{measured}$, the corrected results seem to overpredict the measured discharges.

It is expected that the overpredictions for small values of ${}^{s}q_{measured}$ are due to the fact that the data are situated in the vicinity of the limit of applicability of the quantifier. Suppose the applied scaling procedure provides appropriate correction factors (which is to be studied in more detail), the network should predict values of ${}^{s}q_{NN}$ near 10^{-7}–10^{-8} m^3/s/m for the lowest values of ${}^{s}q_{measured}$. Fig. 3 shows that this value is below the ${}^{s}q$-values on which the quantifier has been trained, i.e. the minimum value in Fig. 3 concerns ${}^{s}q\approx 10^{-7}$ m^3/s/m.

4.4. Application example 4: prototype overtopping at the Zeebrugge breakwater

In Zeebrugge (Belgium) prototype overtopping is measured at a rubble mound breakwater armoured with 25 ton grooved cubes. A picture of overtopping at the Zeebrugge breakwater is given in Fig. 11. Detailed information on the Zeebrugge prototype site and the corresponding measurements is given in Troch et al. (1998) and Geeraerts and Boone (2004).

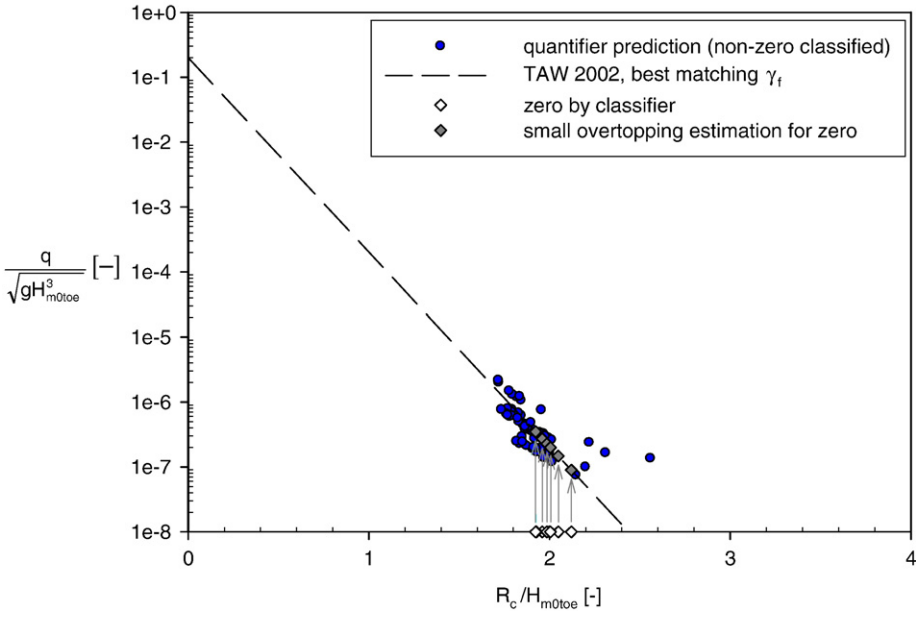

Fig. 9. Small (non-zero) overtopping estimation for zero classified Ostia measurements based on quantifier predictions of non-zero classified Ostia measurements.

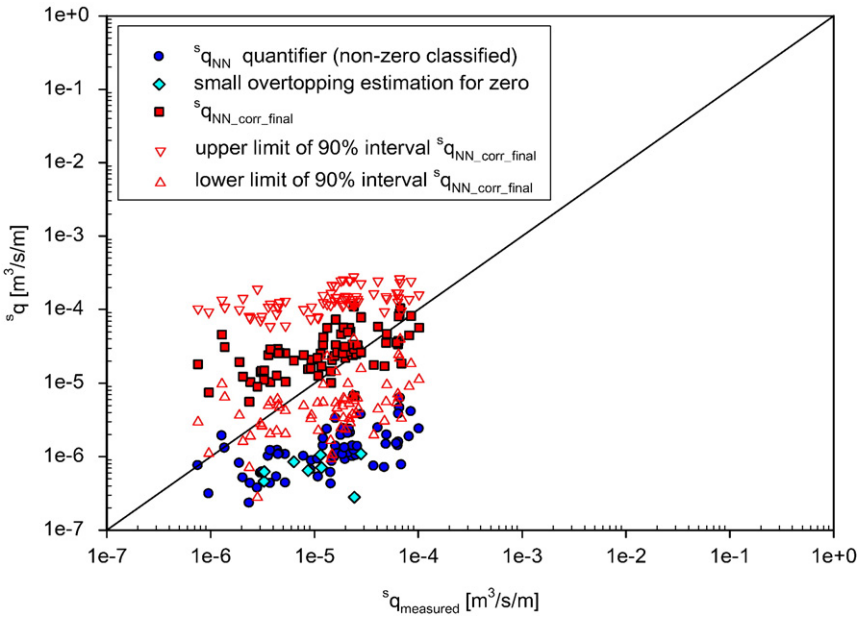

Fig. 10. Combined classifier–quantifier prediction of Ostia measurements.

Between 1999 and 2004, 9 storms with overtopping were recorded, leading to 11 prototype overtopping measurements. The overtopping results are processed per 1 hour (3 data) or per 2 hours (8 data). For the measured mean wave periods $T_{m\ \mathrm{toe}} \approx$ 5.5–6.5 s. This corresponds to processing overtopping events per 550 à 600 waves for the 1 h measurements versus per 1100 à 1300 waves for the 2 h measurements.

The needed scaled hydraulic and structural parameters are determined for all 11 data, leading to values (ranges) of the input parameters for the neural prediction model as summarised in Table 10.

All data fall within the ranges of applicability of the classifier. For one data point the classifier predicts negligible overtopping. For the remaining 10 data, significant overtopping is predicted. Consequently a quantifier simulation of these 10 data is performed. As all 10 data fall within the ranges of applicability of the quantifier, 10 (small scale) overtopping predictions ${}^{s}q_{\mathrm{NN}}$ in $\mathrm{m}^3/\mathrm{s/m}$ are obtained.

The (small scale) predicted values ${}^{s}q_{\mathrm{NN}}$ by the quantifier are corrected with formula (5) for expected model and scale effects,

Fig. 11. Zeebrugge measurement site.

where following value of $f_{\mathrm{scale\_wind}}$ is proposed by De Rouck et al. (2005) for rough, steep breakwater slopes:

$$\text{for } q_{\mathrm{ss}} < 1.10^{-4}\mathrm{m}^3/\mathrm{s/m} : f_{\mathrm{scale\_wind}} = 8$$

$$\text{for } 1.10^{-4} m^3/\mathrm{s/m} \le q_{\mathrm{ss}} \le 1.10^{-2}\mathrm{m}^3/\mathrm{s/m} :$$

$$f_{\mathrm{scale\_wind}} = 1 + 7.\left(\frac{-\log q_{\mathrm{ss}} - 2}{2}\right)^3$$

$$\text{for } q_{\mathrm{ss}} > 1.10^{-2}\mathrm{m}^3/\mathrm{s/m} : f_{\mathrm{scale\_wind}} = 1$$

For the data point classified as negligible overtopping, the procedure to determine a small non-zero prototype overtopping discharge is applied (Fig. 12). The dimensionless armour freeboard $\frac{A_c}{H_{m0\ \mathrm{toe}}} \cong {}^{s}A_c$ is plotted on the x-axis instead of the dimensionless crest freeboard $R_c/H_{m0\ \mathrm{toe}}$, as the maximum armour level is situated higher than the point determining the crest freeboard. The best matching TAW prediction line (TAW, 2002) corresponds to a value of $\gamma_f = 0.60$.

The outcome of the combined classifier–quantifier model for the Zeebrugge data can be summarised as follows (Fig. 13):

- One of the 11 prototype data is assessed by the classifier as resulting in zero or negligible overtopping in small scale tests. A procedure to estimate a small non-zero value for the zero prediction by the classifier is applied, resulting in a value of ${}^{s}q_{\mathrm{ss\_est}} = 1.30 * 10^{-6}\ \mathrm{m}^3/\mathrm{s/m}$.
- Applying a scaling factor $f_{\mathrm{scale\_wind}}$ to the 10 by the quantifier predicted overtopping values q_{NN} and to the single converted zero prediction $q_{\mathrm{ss\_est}}$, results in values of ${}^{s}q_{\mathrm{NN\_corr\_final}}$ as represented in the figure. The rms-error of the final corrected network prediction ${}^{s}q_{\mathrm{NN\_corr\_final}}$ is found to be 0.8442.

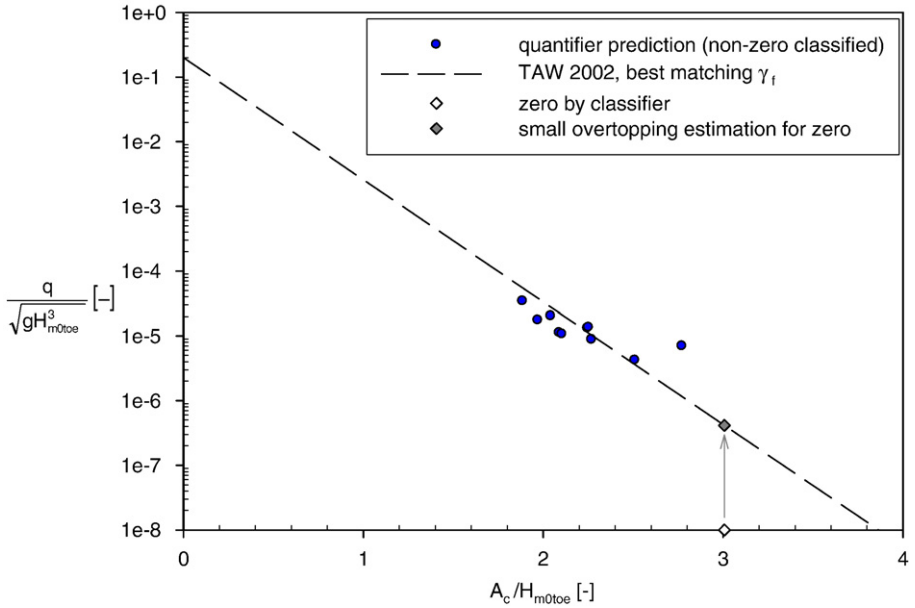

Fig. 12. Small (non-zero) overtopping estimation of zero classified Zeebrugge measurement based on quantifier predictions of non-zero classified Zeebrugge measurements.

- For the final corrected values ${}^{s}q_{NN\_corr\_final}$ originating from the quantifier predictions the 90% intervals are given. They are calculated by correcting the 90% values obtained for the original results ${}^{s}q_{NN}$ for the expected model and scale effects.

Fig. 13 shows that the corrected values ${}^{s}q_{NN\_corr\_final}$ are conservative. For the lowest corrected overtopping discharge ${}^{s}q$ predicted by the quantifier, an overprediction of a factor 31.2 occurs! The overprediction results in a rather large value for the rms-error, i.e. rmse=0.8442. It is not yet clear at this moment what lies on the origin of these overpredictions. As the largest overpredictions occur for the lowest values of ${}^{s}q_{measured}$, the vicinity of the limit of applicability may be noticeable. However, the overpredictions are clearly present for larger values of ${}^{s}q_{measured}$ as well, which raises the question whether the applied scaling procedure is not too conservative for this structure.

5. Discussion and conclusions

The development of a 2-phases neural prediction method for wave overtopping at coastal structures has been presented. The neural prediction method has been trained using an overtopping database in which all structure types are integrated (Verhaeghe, 2005; Van der Meer et al., in press). The result consists of a

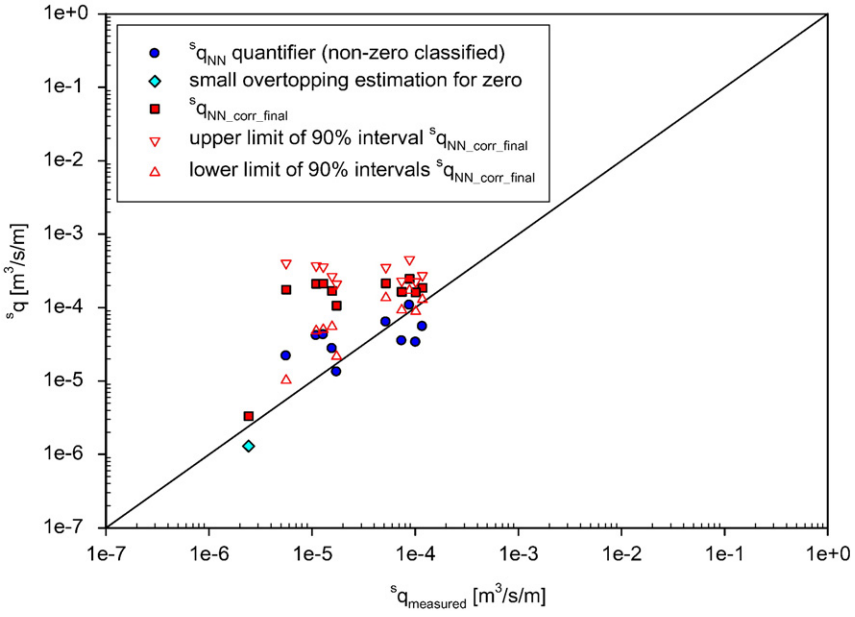

Fig. 13. Combined classifier–quantifier prediction of Zeebrugge measurements.

single model, which is able to predict overtopping at any coastal structure type. It is clear that the overall predictive capacity of the neural prediction method is particularly advantageous. The neural prediction method is composed of 2 subsequent neural networks:

- The 'classifier' predicts whether overtopping occurs or not, i.e. $q=0$ m^3/s/m or $q>0$ m^3/s/m.
- If the classifier predicts overtopping $q>0$ m^3/s/m, then the 'quantifier' is used to determine the mean overtopping discharge, expressed as q in m^3/s/m, i.e. the classifier serves as filter for the application of the quantifier.

Not all of the information included in the database is used for the set-up of the neural prediction method. Large scale overtopping measurements are excluded from the training process of the models, resulting in a prediction method for small scale overtopping. In addition, only 17 of the 31 parameters included in the overtopping database are used for the development of the neural prediction method, i.e.:

- 13 input parameters, consisting of wave parameters and structural parameters,
- 1 output parameter, q in m^3/s/m, which is preprocessed for the quantifier and replaced by 2 discrete values for the classifier,
- 1 scaling parameter used to scale the input parameters, and for the quantifier also the output parameter, according to the Froude model law (to $H_{m0\ toe}=1$ m),
- 2 general parameters, i.e. the reliability factor RF and the complexity factor CF, combined into 1 weight factor, used to force the classifier and quantifier to draw more attention to overall more reliable data.

The gathered information within the CLASH project regarding model and scale effects affecting small scale overtopping measurements, may be used to estimate prototype overtopping discharges corresponding to the small scale neural predictions.

For both classifier and quantifier, a multilayer perceptron with 1 hidden layer is proposed. After the determination of an optimal lay-out for both networks, the bootstrap technique is applied, allowing for the classifier to determine an optimised decision boundary, which is inclined to predict non-zero overtopping in case of doubt (prediction on the safe side). For the quantifier a 'committee of networks' is determined with the bootstrap method. In addition, the bootstrap method results in percentile intervals for the quantifier, providing a certain probability around the point prediction. Application ranges for both classifier and quantifier are set up, which avoids the use of the models outside their ranges of applicability.

It is found that the additional use of the classifier in the prediction method results in a significant improvement over the use of the single quantifier. Due to the filter-effect of the classifier, which is able to distinguish situations where no or negligible overtopping occurs from significant overtopping situations, large overpredictions by the quantifier are avoided.

The developed neural prediction method is validated in section 4 for some specific test series.

The first two test series concern artificial data sets. Overtopping at a rough sloping structure and a vertical wall are studied for a varying dimensionless crest height. Comparison of the combined classifier–quantifier predictions with overtopping discharges estimated with existing empirical models for these artificial data sets shows that the neural prediction method performs very well for the considered structure types. As expected, the percentile intervals are found to be wider in sparsely occupied parts of the input space.

The third and fourth test series concern prototype measurements. The combined classifier–quantifier results obtained for these data are corrected according to expected model and scale effects. For the considered cases, both rough sloping structure types, the combination neural prediction method — applied scaling procedure is found to generally overpredict the smallest measured overtopping discharges. For the Ostia case the overpredictions are rather small and are suggested to originate from the vicinity of the limit of applicability of the quantifier. It may be concluded that a good result is obtained for the Ostia case. For the Zeebrugge case rather large overpredictions are found. It is not clear whether these overpredictions originate from the quantifier prediction or from the scaling factors included in the applied scaling map. Further research on both, the Zeebrugge quantifier predictions and the scaling factors, is therefore advised.

Although it is found that the classifier predicts rather 'safe' overtopping, which was exactly the intention of the decision criterion, it is shown that the combined classifier–quantifier result clearly improves the single quantifier result.

Acknowledgements

The authors would like to acknowledge those who delivered overtopping data for their technical contributions.

The financial contribution of the Research Foundation-Flanders (FWO) is very much acknowledged. A part of this research was performed within the EC-project CLASH (EVK3-CT-2001-00058); the financial contribution of the European Community is also acknowledged.

References

Ahrens, J.P., Heimbaugh, M.S., Davidson, D.D., 1986. Irregular wave overtopping of seawall/revetment configurations, Roughans Point, Massachusetts, USA, final report of experimental model investigation, Coastal Engineering Research Centre, Department of the Army, Mississippi.

Ahrens, J.P., Heimbaugh, M.S., 1988. Seawall overtopping model. Proceedings of the 21st International Conference on Coastal Engineering, Malaga, Spain. ASCE, pp. 795–806.

Allsop, N.W.H., Besley, P., Madurini, L., 1995. Overtopping performance of vertical and composite breakwaters, seawalls and low reflection alternatives. Paper to the final MCS Project Workshop, Alderney, United Kingdom.

Allsop, N.W.H., 2005. Report on hazard analysis, CLASH WP6 report. HR Wallingford, United Kingdom.

Bouma, J.J., Schram, A., François, D., 2004. Report on socio-economic impacts, CLASH WP6 report, Ghent University, Belgium.

De Rouck, J., Geeraerts, J., Troch, P., Kortenhaus, A., Pullen, T., Franco, L., 2005. New results on scale effects for wave overtopping at coastal structures. Proceedings of the ICE Conference on Coastlines, Structures and Breakwaters. London, United Kingdom, pp. 29–43.

Efron, B., 1982. The Jackknife, the Bootstrap and other resampling plans. Society for Industrial and Applied Mathematics. Philadelphia, USA.

Efron, B., Tibshirani, R.J., 1993. An Introduction to the Bootstrap. Chapman & Hall, New York, USA.

Eurotop, 2007. Wave Overtopping of Sea Defences and Related Structures- Assessment Manual. May 2007, www.overtopping-manual.com.

Foresee, F.D., Hagan, M.T., 1997. Gauss–Newton approximation to Bayesian learning. Proceedings of the International Joint Conference on Neural Networks.

Franco, L., De Gerloni, M., Van der Meer, J.W., 1994. Wave overtopping on vertical and composite breakwaters. Proceedings of the 24th International Conference on Coastal Engineering, Kobe, Japan. ASCE, pp. 1030–1045.

Franco, C., Franco, L., 1999. Overtopping formulas for caisson breakwaters with nonbreaking 3d waves. Journal of Waterway, Port, Coastal and Ocean Engineering vol. 125(2), 98–108.

Franco, L., Briganti, R., Bellotti, G., 2004. Report on full scale measurements, Ostia, 2nd full winter season, CLASH WP3 report, Modimar, Rome, Italy.

Franco, L., Geeraerts, J., Briganti, R., Willems, M.L., Bellotti, G., De Rouck, J., in press. Prototype and small-scale model tests of wave overtopping at shallow rubble mound breakwaters: the Ostia-Rome yacht harbour case. Accepted for publication in Special Issue of Coastal Engineering on the CLASH project.

Geeraerts, J., Boone, C., 2004. Report on full scale measurements Zeebrugge, 2nd full winter season, CLASH WP3 report, Ghent University, Belgium.

Goda, Y., 1985. Random seas and design of maritime structures. University of Tokyo Press, Japan0-86008-369-1.

Hornik, K., Stinchcombe, M., White, H., 1989. Multilayer feedforward networks are universal approximators. Neural networks vol. 2, 359–366.

IPCC, 2007. Climate change 2007: The physical science basis. In: Solomon, S., Qin, D., Manning, M., Chen, Z., Marquis, M., Averyt, K.B., Tignor, M., Miller, H.L. (Eds.), Contribution of Working Group I to the Fourth Assessment Report of the Intergovernmental Panel on Climate Change. Cambridge University Press, Cambridge.

Kikkawa, H., Shi-igai, H., Kono, T., 1968. Fundamental study of wave overtopping on levees. Coastal Engineering in Japan vol. 11, 107–115.

Kortenhaus, A., Van der Meer, J.W., Burcharth, H.F., Geeraerts, J., Pullen, T., Ingram, D., Troch, P., 2005. Quantification of measurement errors, model and scale effects related to wave overtopping, CLASH WP7 report, Leichtweiβ Institute for Hydraulics, Technical University of Braunschweig, Germany.

Levenberg, K., 1944. A method for the solution of certain non-linear problems in least squares. Quarterly of Applied Mathematics 2 (2), 164–168.

Marquardt, D.W., 1963. An algorithm for the least-squares estimation of non-linear parameters. SIAM Journal of Applied Mathematics 11 (2), 431–441.

Mase, H., Sakamoto, M., Sakai, T., 1995. Neural network for stability analysis of rubble mound breakwaters. Journal of Waterway, Port, Coastal, and Ocean Engineering vol.121 (6), 294–299.

Medina, J.R., 1998. Wind effects on run-up and breakwater crest design. Proceedings of the 26th International Conference on Coastal Engineering, Copenhagen, Denmark. ASCE, pp. 1068–1081.

Medina, J.R., 1999. Neural network modelling of run-up and overtopping. Proceedings of the International Conference on Coastal Structures, Santander, Spain, pp. 421–429.

Medina, J.R., Gonzalez-Escriva, J.A., Garrido, J., De Rouck, J., 2002. Overtopping analysis using neural networks. Proceedings of the 28th International Conference on Coastal Engineering, Cardiff, United Kingdom. ASCE, pp. 2165–2177.

Owen, M.W., 1980. Design of seawalls allowing for wave overtopping. Report No. EX 924. HR Wallingford, United Kingdom.

Panizzo, A., Briganti, R., Van der Meer, J.W., Franco, L., 2003. Analysis of wave transmission behind low-crested structures using neural networks. Proceedings of the International Conference on Coastal Structures. Portland, USA, pp. 555–566.

Pozueta, B., Van Gent, M.R.A., Van den Boogaard, H.F.P., 2004a. Neural network prediction method. CLASH WP8 Neural Network. Delft Hydraulics, The Netherlands.

Pozueta, B., Van Gent, M.R.A., Van den Boogaard, H.F.P., Medina, J.R., 2004b. Final report on generic prediction method. CLASH WP8 report. Delft Hydraulics, The Netherlands.

Saville Jr., T., 1955. Laboratory data on wave run-up and overtopping on shore structures. TM-64, Beach Erosion Board. US Army Corps of Engineers, USA.

Schüttrumpf, H., 2001. Wellenüberlaufströmung bei Seedeichen- Experimentelle und Theoretische Untersuchungen, Ph.D. Thesis (Wave Overtopping Flow at Seadikes- Experimental and Theoretical Investigations).

Steendam, G.J., Van der Meer, J.W., Verhaeghe, H., Besley, P., Franco, L., Van Gent, M.R.A., 2004. The international database on wave overtopping. Proceedings of the 29th International Conference on Coastal Engineering, Lisbon, Portugal. ASCE, pp. 4301–4313.

TAW, 2002. Technical report wave run-up and wave overtopping at dikes. Technical Advisory Committee on Flood Defence, Author: J.W. van der Meer, The Netherlands.

Troch, P., De Rouck, J., Van Damme, L., 1998. Instrumentation and prototype measurements at the Zeebrugge rubble mound breakwater. Coastal Engineering vol. 35, 141–166 issues 1-2.

U.S. Army Corps of Engineers, 2002. Coastal Engineering Manual, Engineer Manual 1110-2-1100, Washington D.C., USA. (in 6 volumes).

Van der Meer, J.W., Verhaeghe, H., Steendam, G.J., in press. The new wave overtopping database for coastal structures. Accepted for publication in Special Issue of Coastal Engineering on the CLASH project. Database available on: http://www.clash-eu.org.

Van Gent, M.R.A., van den Boogaard, H.F.P., 1998. Neural network modelling of forces on vertical structures. Proceedings of the 26th International Conference Coastal Engineering, Copenhagen, Denmark. ASCE, pp. 2096–2109.

Van Gent, M.R.A., van den Boogaard, H.F.P., Pozueta, B., Medina, J.R., 2007. Neural network modelling of wave overtopping at coastal structures. Coastal Engineering vol. 54 (Issue 8), 586–593.

Van Oosten, R.P., Peixo Marco, J., 2005. Wave transmission at various types of low-crested structures using neural networks, student thesis, Technische Universiteit Delft, Delft, The Netherlands.

Verhaeghe, H., Van der Meer, J.W., Steendam, G.J., 2003. Database on wave overtopping at coastal structures. CLASH WP2 internal report, Ghent University, Belgium.

Verhaeghe, H., 2005. Neural network prediction of wave overtopping at coastal structures, Ph.D. Thesis, Universiteit Gent, Gent, Belgium, ISBN 90-8578-018-7 (available on: http://awww.ugent.be/awww/coastal/verhaeghe2005.html and http://www.clash-eu.org).